

MICROSTRUCTURE-BASED PREDICTION MODEL FOR CHLORIDE ION DIFFUSIVITY IN HYDRATED CEMENT PASTE

#LIGUO MA^{*,**}, YUNSHENG ZHANG^{*}

^{*}School of Materials Science and Engineering, Southeast University, Nanjing, 211189, P.R.China

^{**}School of Civil Engineering, Yantai University, Yantai, 264005, P.R.China

#E-mail: liguomaytu@163.com

Submitted October 24, 2016; accepted December 12, 2016

Keywords: Diffusion coefficient; Microstructure; Hydration products; Homogenization theory; Jennings-Tennis model

In cement hydration, various hydration products and pores are produced to form a complex microstructure. The quantity of the hydration products and pores heavily influences the macroscopic properties of hydrated cement paste. The chloride ion diffusivity of cement paste is considered to have a close relation to durability. We propose a prediction model of the chloride ion diffusivity of cement paste using homogenization theory to find the relationship between the microstructure and the macroscopic properties. This model considers the percolation phenomenon and the tortuosity of the transport path in the hydrated cement paste microstructure. The chloride ion diffusion coefficient of the cement paste was tested via electricity-accelerated diffusion experiments on cement pastes prepared using three water-cement ratios (0.23, 0.35 and 0.53, respectively). The Jennings-Tennis model was used to calculate the quantity of hydration products in the hydrated cement paste microstructure. With different homogenization theories, the predicted results of the chloride ion diffusion coefficients agree well with the experimental data, which shows the reliability of the presented model.

INTRODUCTION

Since its invention, cement has become a vital material in construction and civil engineering due to its many advantages [1, 2]. Its durability has been a popular research topic for many years. Cracks may appear in the concrete in an erosion environment, which adversely affects the performance of concrete, reduces its durability, and shortens its service life [3]. Concrete cracks caused by reinforcement corrosion in chloride environment, concrete damage caused by alkali aggregate reaction, and the concrete failure caused by sulfate expansion are all attributed to durability reduction caused by the transport of corrosive media [4]. Corrosive media for concrete mainly includes pressure water, chloride ions, carbon dioxide and other harmful acids, alkali, or salt solutions. Concrete damage or cracks caused by chloride ions are particularly serious because repairing this damage can be very expensive. Therefore, chloride ion permeability is the key parameter related to the durability of reinforced concrete structures in chloride environments. The quantitative prediction of chloride ion transport performance is important both from the viewpoint of theoretical analysis and practical application.

The cement hydration process is very complicated, and it is difficult to establish a suitable model to describe the cement microstructure consisting of many hydration products and pores [5]. The quantity of hydration products and pores varies with the hydration process, and the hydration products have different contributions

to the transport performance. Pores have a significant impact on transport performance, and previous studies have investigated the effects of pore volume, size distribution, and critical size on transport performance [6], but the effects of other hydration products have not been rigorously studied. More studies focus on the relationship between the microstructure and material properties [7-10]. For example, some works focused on the relationship between the microstructure and cement paste diffusivity. A non-contact electrical resistivity device was used to study the microstructure, and an analytical model was proposed to acquire the relative resistivity of cement paste using an effective medium theory [11]. Numerical simulations of cement paste diffusivity were applied to microcracks caused by tensile loading and frost action [12]. A link between mass diffusivity in cement paste and its microstructure was presented using X-ray computed microtomography for obtaining three-dimensional images of cement paste specimens [13]. A one-dimensional diffusion-based transport model was developed to predict the transport properties of saturated cement pastes using accelerated experimental approaches with changes in the cement paste microstructure [14].

As a heterogeneous material, hydrated cement paste has a variable microstructure consisting of different kinds of hydration products and pores due to cement hydration. In this paper, we establish a quantitative relationship between transport performance and cement paste components to predict cement paste permeability by commonly used homogenization theories, such as

Mori-Tanaka theory and self-consistent theory etc. [15]. The prediction model is built based on the microstructure using homogenization theories to determine cement paste diffusivity.

PREDICTION MODEL BASED ON MICROSTRUCTURE

Hydration process of cement

The production of Portland cement can be summarized in three stages: raw material grinding, clinker burning and cement grinding. The principal production process is clinker burning, with reactions between calcium oxide, silica, alumina, and iron oxide at temperatures of about 1450 °C. The produced anhydrous Portland cement is a gray powder with particles in the size range from 1 μm to 50 μm. The mineral composition of the principal clinker compounds corresponds approximately to C₃S, C₂S, C₃A, and C₄AF using the customary abbreviations in Table 1 [5].

Table 1. Compound or product abbreviations.

Material matrix	Compound or product	Abbreviation
Portland cement clinker	3CaO·SiO ₂	C ₃ S
	2CaO·SiO ₂	C ₂ S
	3CaO·Al ₂ O ₃	C ₃ A
	4CaO·Al ₂ O ₃ ·Fe ₂ O ₃	C ₄ AF
Cement paste	hydration products	HP
	calcium silicate hydrate	C-S-H
	calcium hydroxide	CH
	monosulfoaluminate hydrate	AFm
	ettringite	AFt
	calcium ferrite hydrate	C-F-H
	calcium aluminate hydrate	C-A-H
unhydrated cement core	UC	

Portland cement is dispersed in water. The cement particles dissolve partially, and the liquid phase is saturated with various ions. Several minutes after cement hydration, the calcium trisulfoaluminate hydrate called ettringite appears (abbreviated AFt). A few hours later, calcium hydroxide (CH) and calcium silicate hydrates (C-S-H) begin to fill the space originally occupied by

water and the partially dissolved cement particles. After a few days, AFt becomes unstable and decomposes to form monosulfoaluminate hydrate (AFm) according to the ratio of alumina to sulfate. Calcium aluminate hydrates (C-A-H) are formed in the hydrated pastes of either undersulfated or high-C₃A Portland cements. Calcium ferrite hydrate (C-F-H) also appears according to the C₄AF content. Aluminum- or iron-containing phases such as C-A-H, AFt, AFm and C-F-H etc. are referred to as AF in the paper. The abbreviations of hydration products are listed in Table 1 [16].

When the Portland cement particles are dispersed in water, the distance between the cement particles is large and the hydration products are attached to the surface of the particles. As hydration continues, the hydration products multiply and begin to mix and interlace. The distance between particles becomes shorter and the cement paste loses macroscopic plasticity gradually. The hydration products slowly coagulate and overlap due to the shortened distance between the cement particles. Finally, the cement paste completely loses its plasticity and reaches a state of final setting, resulting in structural strength. There are many pores between the hydration products in the hydrated paste. The hydration reaction gradually proceeds from the surface to the interior of the cement particles, but with the increase and accumulation of hydration products on the surface, it becomes more difficult for water to penetrate into the interior of the cement particles. The unhydrated cement core (UC) still exists in most of the cement particles for months or even years after the beginning of cement hydration. Figure 1 shows the cement setting and hardening process.

Various phases in the cement hydration process form a complex microstructure in the hardened cement paste, which mainly includes CH, C-S-H, C-A-H, AFt, AFm, C-F-H, pores and UC. According to previous studies, C-S-H can be divided into two types: low density C-S-H (LD C-S-H) and high density C-S-H (HD C-S-H) [17, 18]. In the hydrated cement paste microstructure, the various phases can be divided into two types, viz. permeable and non-permeable phases according to different diffusivity contributions. The permeable phases include two types of C-S-H and pores. The non-permeable phases mainly include CH, AF and UC.

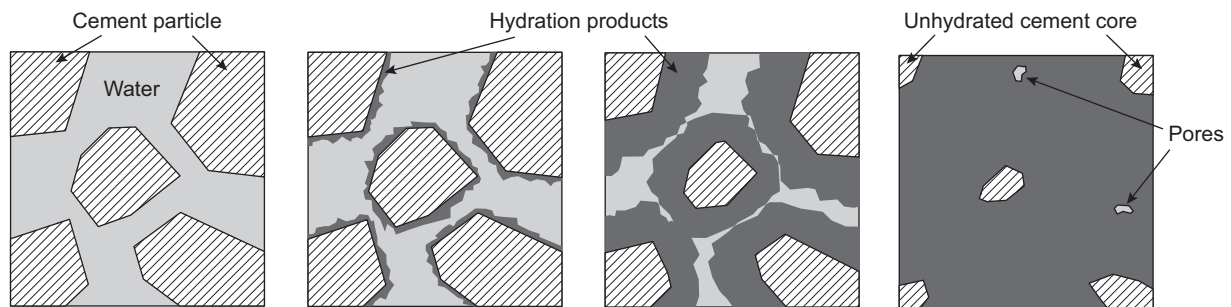


Figure 1. Cement setting and hardening process (schematic).

Formulation of the microstructure-based prediction model

Hardened cement paste microstructures consist of various phases with different diffusivity contributions. The volume fractions of the phases and other parameters were considered to establish a quantitative prediction model using different homogenization theories in combination. The prediction model was described with a step-by-step flow chart detailed in Figure 2 from a microscopic to a macroscopic view.

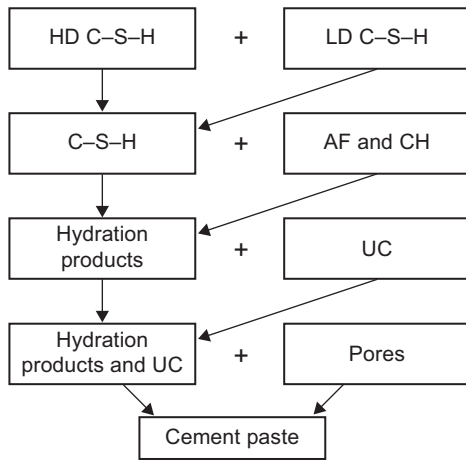


Figure 2. Prediction model flow chart.

Combination of HD C-S-H and LD C-S-H

According to density differences, C-S-H can be divided into HD C-S-H and LD C-S-H [18]. In the combination of C-S-H without considering the gel pores of C-S-H (due to its low content), the two types of C-S-H are simulated as a multilayer composite sphere with an inner core of HD C-S-H and outer shell of LD C-S-H, called a simply coated sphere assemblage formulation. The effective diffusion coefficient of this C-S-H combination can be calculated by the generalized self-consistent theory, as expressed in Equation 1 and Equation 2 [15]. Figure 3 illustrates the combination model.

$$D_{C-S-H} = d_{LDC-S-H} + (1 - \xi)[(d_{HDC-S-H} - d_{LDC-S-H})^{-1} + \frac{\xi}{3d_{LDC-S-H}}]^{-1} \quad (1)$$

$$\xi = \phi_{LDC-S-H}(\phi_{LDC-S-H} + \phi_{HDC-S-H})^{-1} \quad (2)$$

In equation (1), the d are the phase diffusion coefficients of the phases in the C-S-H combination and D_{C-S-H} is the effective diffusion coefficient of C-S-H; in equation (2), ϕ are the volume fractions of phases in the C-S-H combination.

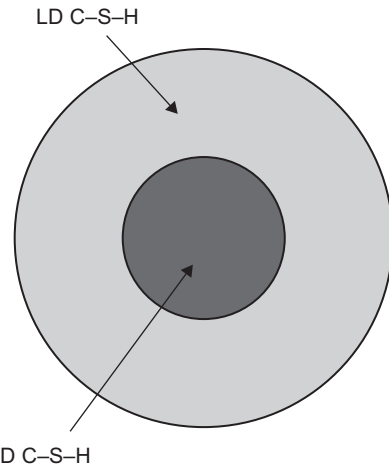


Figure 3. Combination model of LD C-S-H and HD C-S-H.

Combination of C-S-H, AF and CH

Besides HD C-S-H and LD C-S-H, there are phases of AF and CH mixed with C-S-H to form HP. In this combination, the effective diffusion coefficient can be calculated using the Mori-Tanaka homogenization theory, which is suitable for non-permeable phases embedded in a permeable matrix, as expressed in Equation 3 and Equation 4 [15]. Figure 4 shows the combination model.

$$D_{HP} = 2D_{C-S-H} (1 - \phi_{CH+AF}) (2 + \phi_{CH+AF})^{-1} \quad (3)$$

$$\phi_{CH+AF} = \frac{V_{CH+AF}}{V_{CH+AF} + V_{C-S-H}} \quad (4)$$

In Equation 3, D_{HP} is the effective diffusion coefficient of the combination of the hydration products, while D_{C-S-H} is obtained from Equation 1. In Equation 4, V are volumes of phases.

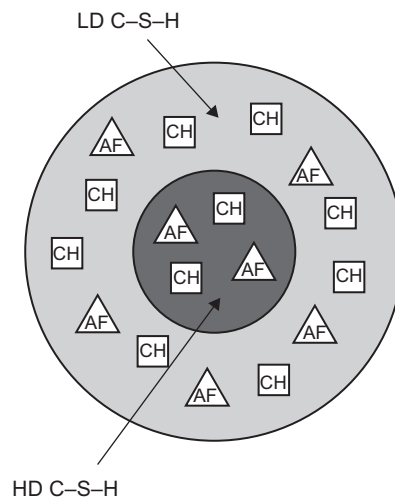


Figure 4. Combination model of hydration products.

Combination of HP and UC

In the hydration process, cement hydration starts from the surface of cement particles and gradually propagates into the interior, while the unhydrated cement core still remains in the interior of cement particles. It can be simplified as a combination sphere with an inner UC and an outer layer of HP, which can also be calculated analogous to Equation 1 and Equation 2. Figure 5 shows the combination model.

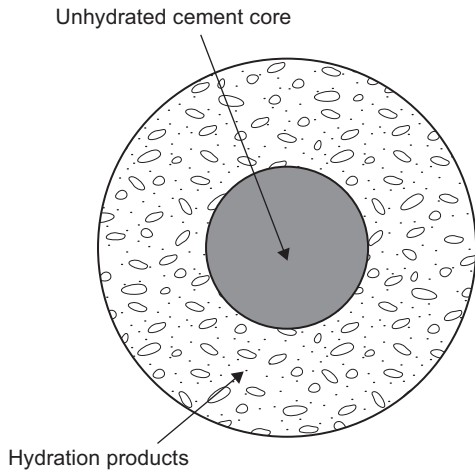


Figure 5. Combination model of unhydrated cement core and hydration products.

Combination of HP, UC and pores

Hardened cement paste, including hydration products (HP), unhydrated cement core (UC) and pores, can be simplified as a combination of pores mixed in HP and UC, as shown in Figure 6.

In combination (HP, UC, and pores), hardened cement paste can be considered as a composite material with two different phases that have very different effects on the material's effective diffusivity. Phase

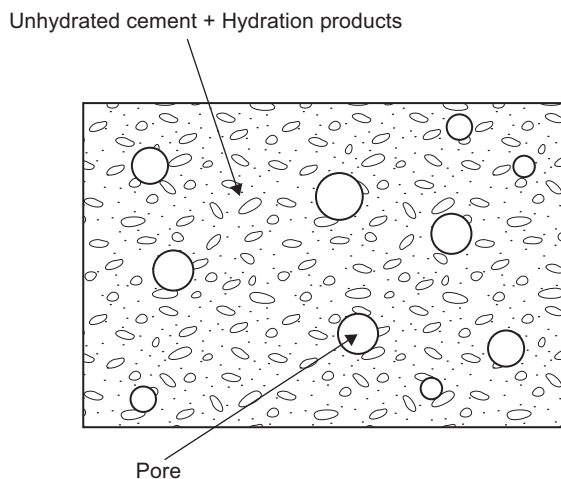


Figure 6. Combination model of HP, UC and pores.

1 is the combination of HP and UC, referred to as the solid phase, while phase 2 is the pore phase. The two phases have different diffusion coefficients, that of the pore, d_{pore} being much larger than that of the solid, d_{solid} . Usually part of the pore phase exhibits the phenomenon of percolation. This is the case, the percolating part of the pore phase can be arranged in parallel with the combination of the non-percolating part of the pore phase and solid phase in the model, while the non-percolating part of the pore phase can be viewed as being connected with the solid phase in series. In the parallel case, diffusion is controlled by the volume fraction of the percolating part of the pore phase, while in the series case, it is controlled by the solid phase and the non-percolating part of the pore phase.

The tortuosity coefficient is introduced to reflect the three-dimensional geometry of the phases in hardened cement paste. Hereby it is assumed that the composite material consists of two phases. One is an almost non-permeable matrix phase (solid), while the other is more permeable (pore phase). The more permeable phase must enable transport through a connected path, and the tortuosity coefficient thus reflects the length of the diffusion path or the formation difficulty of the diffusion path, as shown in Figure 7. Thus the effective diffusion coefficient of the composite material depends on the tortuosity coefficients, the phase diffusion coefficients and the phase volume fractions, as expressed in Equation 5 [19].

$$\frac{D_e}{d_i} = \frac{\phi_i}{T_i(\phi_i)} \quad (5)$$

In Equation 5, D_e is the effective diffusion coefficient of the composite material, d_i are the phase diffusion coefficients (of solid and pore phase), ϕ_i are the volume fractions of (solid and pore phase) and $T_i(\phi_i)$ are the tortuosity coefficients (of solid and pore phase) as a function of the respective volume fractions ϕ_i .

In the literature, an exponential relation for the pore tortuosity coefficient for inclusions embedded in a matrix has been successfully applied in hardened cement paste, as expressed in Equation 6 [20], where $T_{(\phi)}$ is the pore tortuosity coefficient and ϕ the pore volume fraction (porosity).



Figure 7. A scheme for explaining tortuosity.

$$T_{(\phi)} = [0.0067 \exp(5.0\phi)]^{-1} \quad (6)$$

According to the study cited [20], the tortuosity coefficient of the matrix or the combination of the matrix and other phases approximately equals 1. The percolation phenomenon reflects the fact that the volume fraction of the more permeable phase has a threshold above which a continuous transport path occurs, as shown in Figure 8. When the volume fraction of the more permeable phase is lower than the threshold, the transport path is impassable. On the other hand, as long as the volume fraction of the more permeable phase exceeds the threshold it will form a continuous transport path. Figure 9 illustrates the percolation function of the more permeable phase, i.e. the dependence of the percolating fraction on the total volume fraction, in hardened cement paste [19].

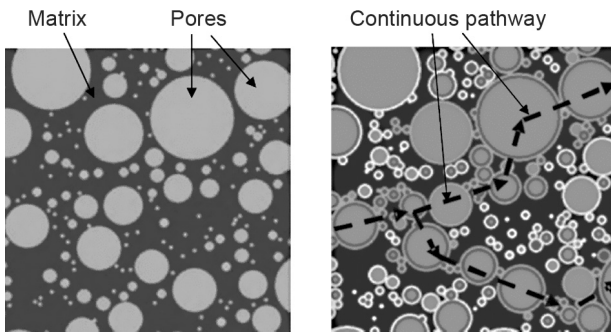


Figure 8. Percolation phenomenon.

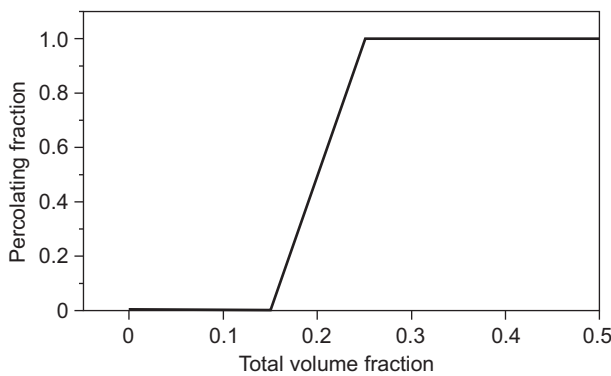


Figure 9. Percolation function of the diffusing pore phase.

When the volume fraction of the percolating part of the pore phase is y , the effective diffusivity of the combination of the two phases (solid and pore phase) can be calculated by Equation 7 [19].

$$D_e = [y\phi_{pore}d_{pore} \frac{1}{T_{(y\phi_{pore})}}] + [(1-y)\phi_{pore} + \phi_{solid}] \quad (7)$$

$$\left[\frac{(1-y)\phi_{pore} + \phi_{solid}}{\left(\frac{(1-y)\phi_{pore}}{d_{pore}} + \frac{\phi_{solid}}{D_{solid}}\right)} \right] \left[\frac{1}{T_{(\phi_{solid} + (1-y)\phi_{pore})}} \right]$$

When the pore phase is completely percolating, the model is a pure parallel model. On the contrary, when the volume fraction of the pore phase does not reach the percolation threshold, the model is a pure series model.

In the prediction model presented here, the diffusion coefficient of the completely impermeable phases (CH, AF and UC) are not considered. The diffusion coefficients of HD C-S-H ($d_{HD \text{ C-S-H}}$), LD C-S-H ($d_{LD \text{ C-S-H}}$) and the pore phase (d_{pore}) are assumed to be $8.3 \times 10^{-13} \text{ m}^2/\text{s}$, $3.4 \times 10^{-12} \text{ m}^2/\text{s}$ and $2.0 \times 10^{-9} \text{ m}^2/\text{s}$, respectively [19].

In the hardened cement paste prediction model, HP and UC are the matrix and the mixed component are pores with the percolation phenomenon shown in Figure 10. When the water-cement ratio is low, the pores do not percolate in the system because their volume fraction does not reach the percolation threshold. In this case the pores are connected in series with HP and UC, as shown in part (1) of Figure 11. When the water-cement ratio is large enough for some pores to percolate, the percolating fraction of the pores is parallel with the combination of the non-percolating part of pores, HP and UC. In this case, the non-percolating part of pores is connected in series with HP and UC, as shown in part (2) of Figure 11. When the water-cement ratio is large enough for the pores to percolate completely, the pores are in parallel with HP and UC, as shown in part (3) of Figure 11.

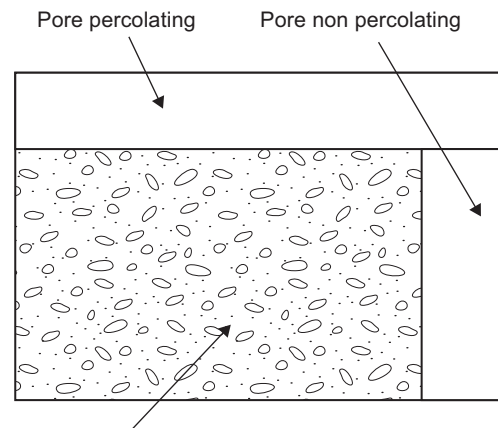


Figure 10. Arrangement of percolation effect.

In order to obtain a more precise description of the C-S-H matrix in cement pastes, C-S-H can be described according to the Jennings-Tennis model, which considers two types of C-S-H phases, low-density (LD) C-S-H, and high-density (HD) C-S-H [17, 18]. These two C-S-H types and the pores are considered in a homogenization model to estimate cement paste diffusivity. The Jennings-Tennis model was used to determine the volume fraction of the individual phases in the hardened cement paste. Thus the volume fractions of hydration products and pores can be determined for the prediction model calculation.

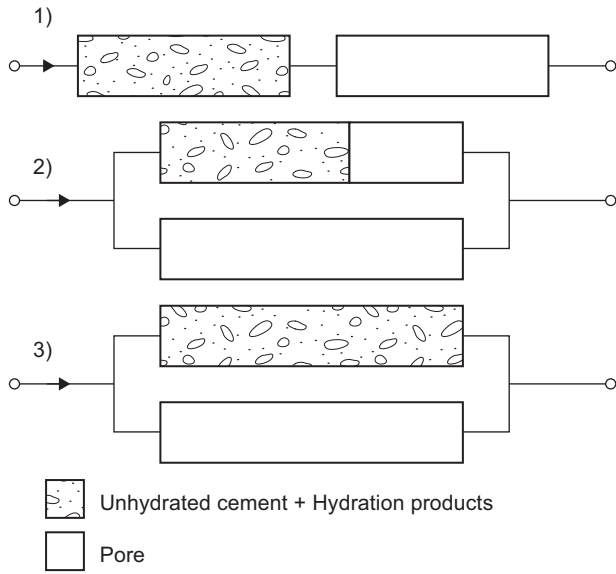


Figure 11. Series model and parallel model.

EXPERIMENTAL

Materials

To validate the accuracy of the prediction model, experiments were designed to obtain the chloride ion diffusion coefficient of cement pastes. This experiment used 52.5 Grade Portland cement with a specific surface of 369.6 m²/kg supplied by the Huaxin Cement Company of Hubei province in China. Table 2 presents the cement composition. Water-cement ratios of 0.23, 0.35 and 0.53, commonly used in practical engineering, were used for preparing the cement pastes of these experiments.

Table 2. Composition of the cement used.

Chemical composition	Content (mass %)
SiO ₂	21.35
CaO	62.6
Fe ₂ O ₃	3.31
Al ₂ O ₃	4.67
MgO	3.08
TiO ₂	0.27
SO ₃	2.25
Loss on ignition	0.95

Experimental instrument and process

The specimens of the hardened cement paste were kept in standard curing conditions for 28 days and 90 days, respectively. The specimens were shaped as cylinders with 100 mm diameter and 50 mm height. The experimental equipment used in the electricity-accelerated diffusion experiment was made with a chloride ion diffusion medium and operated according to the NT BUILD 355 standard [21], as shown in Figure 12.

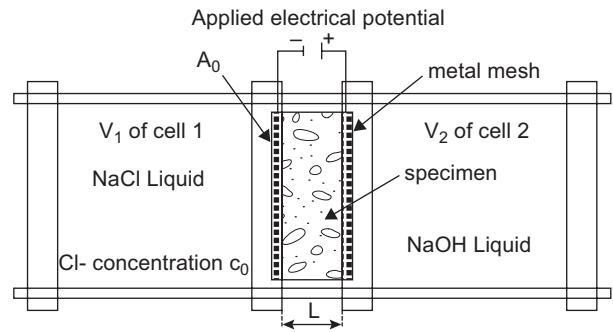


Figure 12. Schematic diagram of electricity-accelerated diffusion experiment.

As shown in Figure 12, the chloride ions from cell 1 are driven to cell 2 by the applied electrical potential. When the change of chloride ion diffusion in cell 2 is in a steady state, the chloride ion diffusion coefficient (m²/s) of the specimens is calculated via Equation 8 [22].

$$D = 300 \frac{kT}{ze_0 \Delta \varphi} \frac{VL}{c_0 A_0} \frac{dc}{dt} \quad (8)$$

In this equation (Equation 8) *k* is the Boltzmann constant (1.8×10⁻²³ J/K), *T* the absolute temperature (K), *z* the valence of the chloride ion, *e*₀ the electron unit charge (1.60×10⁻¹⁹ C), Δ*φ* the applied electrical potential, *L* the distance between the two electrodes, *V* the volume of cell 2, *c*₀ the chloride concentration in cell 1, *A*₀ the cross section area of the electrodes and *dc/dt* the chloride concentration change rate of chloride ions in cell 2.

Figure 13 shows the equipment and process of the electricity-accelerated diffusion experiment corresponding to the schematic diagram given in Figure 12. In the experimental process many specimens are tested simultaneously with DC power supply.

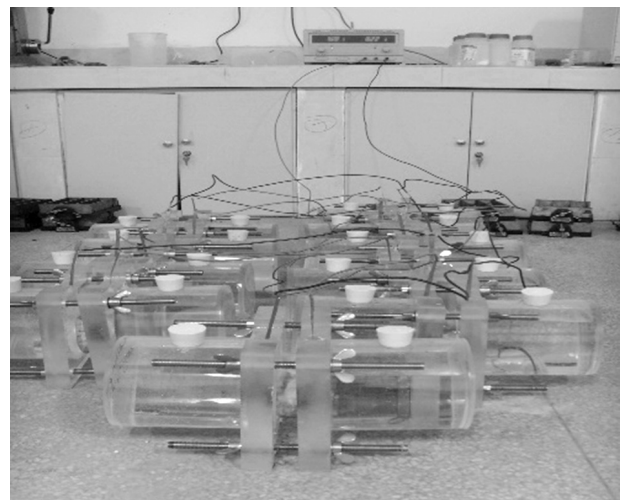


Figure 13. Equipment and process of electricity-accelerated diffusion experiments.

RESULTS AND DISCUSSION

The volume fractions of hydration products, pores and unhydrated cement core of the hardened cement pastes (after curing for 28 days and 90 days, respectively) were calculated through the Jennings-Tennis model, as shown in Table 2. The calculated volume fractions were used as input data into the presented model to predict the chloride ion diffusion coefficient. Figure 14 shows the chloride ion diffusion coefficient of the hardened cement pastes obtained from the electricity-accelerated diffusion experiments, and the presented model results for curing time of 28 days and 90 days, respectively. Comparing Figures 14a and 14b, the chloride ion diffusion coefficient after 90 days curing was smaller than that after 28 days curing. The reason is that during curing the amount of hydration products increases and the cement paste becomes denser. The change of the hydration products can be obtained from Table 3. In the presented model, the necessary parameters mainly include the volume fractions and the phase diffusion coefficients of the components in the hardened cement paste microstructure. The different component quantities and properties have remarkable effects on the chloride ion diffusion coefficient of the hardened cement paste, which confirms that the microstructure is the basic factor influencing the macroscopic performance. In the model, the combination of LD C-S-H and HD C-S-H, as

well as the combination of AF, HP and UC, is basically reasonable, because it corresponds to the real cement hydration process. After the addition of pores in the model, series and parallel combinations are used to take into account the percolation phenomenon. Both the percolation threshold and the tortuosity coefficient were added to the presented model to modify the model by considering the percolation and tortuosity of the pore path in the 3D microstructure of the hardened cement paste. In the experiments, different water-cement ratios of 0.23, 0.35 and 0.53, corresponding to low-, medium- and high-strength concretes, commonly used in practical engineering, were selected to verify the presented model. The water-cement ratio is one important factor in cement hydration. In the hydration process, the water-cement ratio can change the relative volume ratio between the hydration products and pores. In the presented model, the basic input parameters include the volume fractions of the various components, which will finally affect the chloride ion diffusion coefficient of cement paste. There is a macroscopic correlation between the chloride ion diffusion coefficient and the water-cement ratio, which is essentially due to the changing cement paste microstructure as a function of the water-cement ratio.

According to the comparison between the experimental and model results, the chloride ion diffusion coefficient increases similarly as the water-cement ratio increases, as shown in Figure 14. The model results

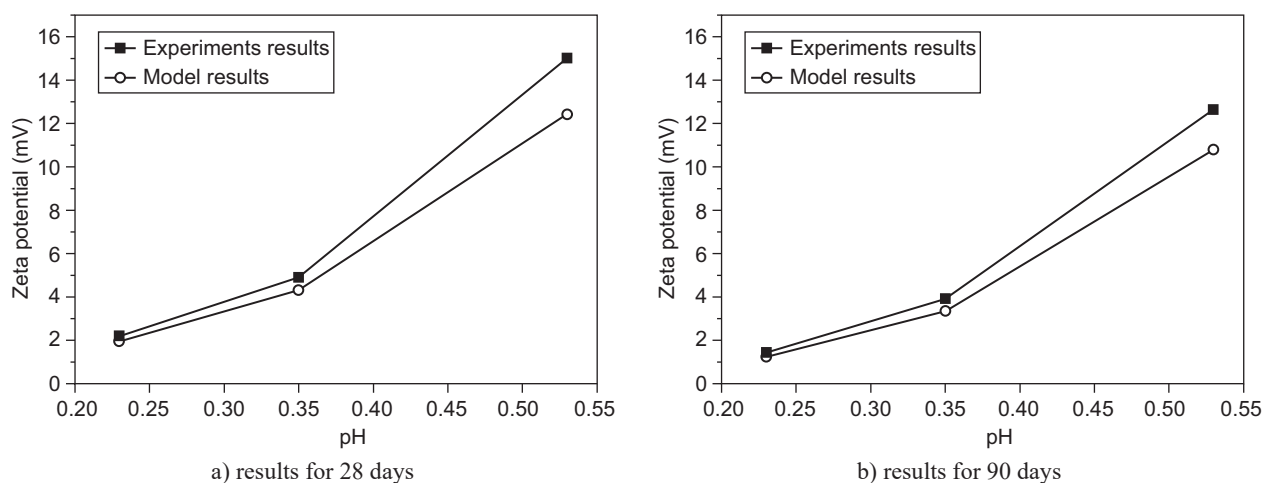


Figure 14. Comparison between experiments results and model prediction results for cement paste hardened for 28 days and 90 days.

Table 3. Volume fractions of phases in hardened cement paste, calculated via the Jennings-Tennis model (%).

w/c	t/d	HD-CSH	LD-CSH	AF	CH	Pores	UC	HP
0.23	28	27.64	9.40	14.93	10.58	7.82	29.63	62.55
	90	30.23	9.08	16.43	11.33	5.12	27.81	67.07
0.35	28	21.95	16.17	18.56	10.40	14.04	18.88	67.08
	90	26.42	17.39	18.18	11.63	11.66	14.72	73.62
0.53	28	8.67	32.00	18.07	10.80	24.84	5.62	69.54
	90	8.69	33.79	18.95	11.16	23.22	4.19	72.59

are consistent with the experimental result trends. For specimens cured for 28 days, the relative differences between experimental and model results of the specimens with water-cement ratios of 0.23, 0.35 and 0.53 were 11.1 %, 12.4 % and 17.3 %, respectively (average relative deviation 13.6 %), while for specimens cured for 90 days, the differences between experimental and predicted results of the specimens with water-cement ratios of 0.23, 0.35, and 0.53 were 9.4 %, 13.2 % and 14.3 %, respectively (average relative deviation 12.2%). Thus, roughly speaking, the prediction model accuracy is around 10 %, which is basically equivalent to the results of other research works that compare measured and predicted results [12, 14]. Overall, the predicted model results agree well with the experimental results, so it seems reasonable to use this model based on homogenization theories. Of course, the difference between the experimental and predicted results may also be caused by the accuracy of the input parameters of the model. Therefore it would be desirable to verify these through additional experimental tests, such as tests on the percolation threshold and the tortuosity coefficient.

CONCLUSIONS

The complicated cement microstructure is formed during the cement hydration process. Microstructure components have a great influence on the macro-performance of hardened cement paste. The diffusion coefficient of chloride ions is particularly important for the durability of cement. Therefore this paper establishes a microstructure-based prediction model aiming at linking properties like the quantity and features of components in the cement paste microstructure with the chloride ion diffusion coefficient in hardened cement pastes. In the model the main input parameters include the volume fraction and the diffusion coefficient of each phase. In addition, the pore percolation effect and the tortuosity coefficient of the diffusion medium chloride ion pathway are considered. In the presented model homogenization theories were used to simplify the combination of the components in the hardened cement paste microstructure. In order to validate the accuracy and suitability of the presented model, experiments were carried out to compare experimental results and model predictions. The comparison shows that the predicted model results agreed well with the experimental data. The difference between the experimental and model results for the chloride ion diffusion coefficients after 28 and 90 days are between 9.4 % to 17.3 %, which is an acceptable agreement. The accuracy of the prediction model could be improved by more precise input parameters, and further experiments may modify the parameters in order to extend the applicability of the model to cement pastes with mineral admixtures.

Acknowledgements

The research work is supported by the National Basic Research Program of China (973 Program: 2015CB655100).

REFERENCES

1. Metha P. K., Monteiro P. J. M. (2006). *Concrete: Microstructure, Properties, and Materials*. 3rd ed. McGraw Hill.
2. Bensted J., Barnes P. (2002). *Structure and Performance of Cements*. Spon Press.
3. Bird R. B., Warren E. W., Lightfoot E. N. (2006). *Transport Phenomena*. John Wiley & Sons Inc.
4. Richardson M. G. (2002). *Fundamentals of Durable Reinforced Concrete*. CRC Press.
5. Taylor H. F. W. (1997). *Cement Chemistry*. Thomas Telford Publishing.
6. Tumidajski P., Schumacher A. S., Perron S., Gu P., Beaudoin J. J. (1996): On the relationship between porosity and electrical resistivity in cementitious systems. *Cement and Concrete Research*, 26, 539–544. doi: 10.1016/0008-8846(96)00017-8
7. Mainguy M., Tognazzi C., Torrenti J. M., Adenot F. (2000): Modeling of leaching in pure cement paste and mortar. *Cement and Concrete Research*, 30, 83–90. doi: 10.1016/S0008-8846(99)00208-2
8. Ma H. Y., Hou D. S., Li Z. J. (2015): Two-scale modeling of transport properties of cement paste: Formation factor, electrical conductivity and chloride diffusivity. *Computational Materials Science*, 110, 270-280. doi:10.1016/j.commatsci.2015.08.048
9. Han J., Wang K. (2016): Influence of bleeding on properties and microstructure of fresh and hydrated Portland cement paste. *Construction and Building Materials*, 115, 240-246. doi:10.1016/j.conbuildmat.2016.04.059
10. Du X., Jin L, Zhang R, Li Y. (2015): Effect of cracks on concrete diffusivity: A meso-scale numerical study. *Ocean Engineering*, 108, 539-551. doi:10.1016/j.oceaneng.2015. 08.054
11. Liu Z, Zhang Y, Liu L, Jiang Q. (2013): An analytical model for determining the relative electrical resistivity of cement paste and C-S-H gel. *Construction and Building Materials*, 48, 647-655. doi:10.1016/j.conbuildmat.2013.07.020
12. Liu L., Chen H., Sun W., Ye G. (2013): Microstructure-based modeling of the diffusivity of cement paste with micro-cracks. *Construction and Building Materials*, 38, 1107-1116. doi: 10.1016/j.conbuildmat.2012.10.002
13. Zhang M., He Y., Ye G., David A. L, Breugel K. V. (2012): Computational investigation on mass diffusivity in Portland cement paste based on X-ray computed microtomography (μ CT) image. *Construction and Building Materials*, 27, 472-481. doi: 10.1016/j.conbuildmat.2011.07.017
14. Quoc T. P, Norbert M., Diederik J., Janez P., Geert D. S., Ye G. (2016): Modelling the evolution of microstructure and transport properties of cement pastes under conditions of accelerated leaching. *Construction and Building Materials*, 115, 179-192
15. Torquato S. (2001): *Random Heterogeneous Media: Microstructure and Macroscopic Properties*. Springer Science & Business Media.

16. Powers T. C. (1958): *The Physical Structure and Engineering Properties of Concrete*. PCA Bulletin.
 17. Jennings H. M. (2000): A model for the microstructure of calcium silicate hydrate in cement paste. *Cement and Concrete Research*, 30, 101-116.
doi:10.1016/S0008-8846(99)00209-4
 18. Tennis P., Jennings H. M. (2000): A model for two types of calcium silicate hydrate in the microstructure of Portland cement pastes. *Cement and Concrete Research*, 30, 855-863. doi:10.1016/S0008-8846(00)00257-X
 19. Bejaoui S., Bary B. (2007): Modeling of the link between microstructure and effective diffusivity of cement pastes using a simplified composite model. *Cement and Concrete Research*, 37, 469-480.
doi:10.1016/j.cemconres.2006.06.004
 20. Mainguy M., Tognazzi C., Torrenti J. M., Adenot F. (2000): Modeling of leaching in pure cement paste and mortar. *Cement and Concrete Research*, 30, 83-90.
doi: 10.1016/S0008-8846(00)00257-X
 21. Nordtest method 1997 NT BUILD 335. (1997). *Chloride diffusion coefficient from migration cell experiments*. Espoo Finland.
 22. Zhang T. and Odd E. G. (1994): An electrochemical method for accelerated testing of chloride diffusivity in concrete. *Cement and Concrete Research*, 24, 1534-1548.
doi:10.1016/0008-8846(94)90168-6
-